# Giant modulation of antiferromagnetic spin reversal field by magnetoelectric effect

Antiferromagnetic (AFM) materials exhibit no net magnetization because magnetic moments are fully compensated within the chemical unit cell. This inherent feature provides robustness of the AFM spin states against magnetic field perturbations. This feature is used in spintronic devices to define the reference magnetic layer. In other words, the functionality of AFM materials is static, and the dynamic control of AFM spins remains a considerable challenge. Spintronics is a research field that aims to control the magnetic moment based on the interplay between spin and charge. An object to be controlled in spintronics is not limited to spontaneous magnetization; the AFM materials also become the target of spintronics. The magnetoelectric (ME) effect is referred to as electric polarization ($\boldsymbol{P}$) by a magnetic field ($\boldsymbol{H}$) and magnetization ($\boldsymbol{M}$) induced by an electric field ($\boldsymbol{E}$) through ME susceptibility $\alpha$: $\Delta\boldsymbol{P} = \alpha\cdot\boldsymbol{H}$ and $\Delta\boldsymbol{M} = {}^{t}\alpha\cdot\boldsymbol{E}$. As illustrated in Fig. 1(a), $E$ increases or decreases the expectation value of $\langle m_z \rangle$ of two spin sublattices, yielding a finite $\Delta\boldsymbol{M}$. $\alpha$ is nonzero in materials in which the spatial- and time-inversion symmetries are simultaneously broken. Because spatial inversion symmetry is inherently broken at the surface/interface, the surface of ME materials exhibits a spin-polarized FM-like state called boundary magnetization (BM) [1]. $Cr_2O_3$ is a prototypical ME-AFM material, and the presence of the BM on $Cr_2O_3$ (0001) was predicted based on symmetry arguments. The BM couples to the bulk AFM order parameter, and the magnitude can be a few orders of magnitude larger than the attainable magnetization owing to the bulk ME effect. Because BM localizes at the surface or the interface with another layer, reducing the ME layer thickness is a valid and feasible way to effectively use BM. To experimentally access the BM, we developed a detection technique based on interfacial spin-dependent transport, for example, the anomalous Hall effect (AHE) at heavy-metal/ME-AFM interfaces such as Pt/$Cr_2O_3$ [2]. In this study, we investigated voltage control of the BM in a Pt/$Cr_2O_3$/Pt epitaxial trilayer. We demonstrated the giant modulation efficiency of the switching field of the order of a few T·nm/V [3].

Figure 1(b) shows the magnetic-field dependence of the AHE resistance $R_{xy}$ for the Pt (2 nm)/$Cr_2O_3$ (8 nm)/Pt (20 nm) epitaxial trilayer. The device structure was designed such that the sense current flowed into the top Pt (2 nm) layer. Rectangular hysteresis was observed, indicating isothermal and reversible switching of the BM. The switching field $\mu_0 H_{SW}$, 600 mT at zero $V_G$, decreased with increasing $V_G$. Under the $V_G$ application, the rectangular shape was maintained. To ensure voltage-induced modulation of the switching field, we measured the $V_G$-dependence of $R_{xy}$ while maintaining the magnetic field strength. After introducing the spin state into that with negative $R_{xy}$, we measured $R_{xy}$ while sweeping $V_G$ at −0.58 T. As shown in Fig. 1(c), $R_{xy}$ switched from negative to positive at $V_G$ = 55 mV, supporting the $V_G$-induced modulation of the switching field. The detailed $V_G$ dependence of the switching field (Fig. 1(d)) showed the monotonic decrease of the switching field in the $V_G$ range from −0.3 V to +0.3 V. Roughly assuming the linear relationship between $\mu_0 H_{SW}$ and $V_G$, the modulation efficiency $\Delta\mu_0 H_{SW}/\Delta V_G$ was −180 mT/V, corresponding to −1400 mT·nm/V. Notably, the temperature dependence of the modulation efficiency yielded the highest value of −500 mT/V (−4800 mT·nm/V). These values are 50 times larger than those of the FM counterpart based on the voltage-controlled magnetic anisotropy (VCMA) effect.

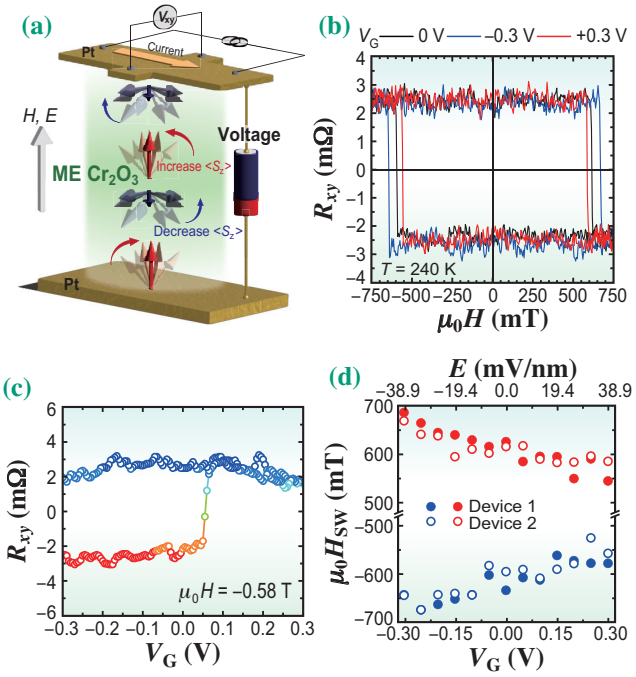


Fig. 1. **(a)** Schematic of a device structure of magnetoelectric (ME) $Cr_2O_3$ equipped with Pt gate electrodes. Voltage application impacts the bulk spin state via the ME effect. **(b)** $R_{xy}$ as a function of $\mu_0 H$ under the application of $V_G$. **(c)** $R_{xy}$ as a function of $V_G$ at a constant $\mu_0 H$. **(d)** $\mu_0 H_{SW}$ as a function of $V_G$ and electric field $E$ (referred to as the top axis).

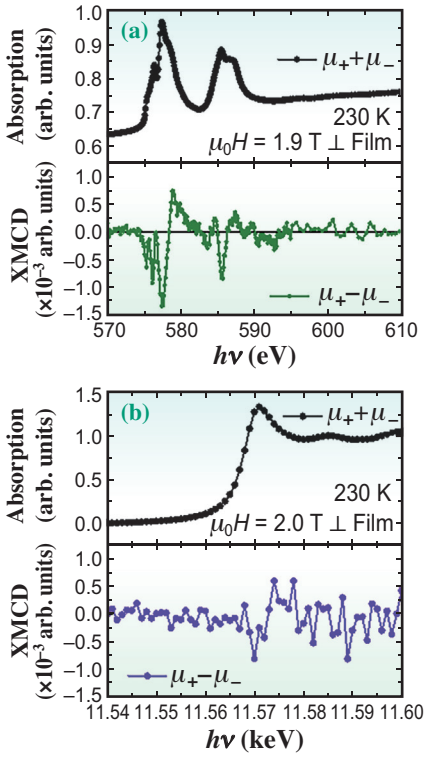


Fig.2. XAS and XMCD spectra at **(a)** Cr $L_{2,3}$ and **(b)** Pt $L_3$ edges, respectively.

To address the microscopic origin of the huge modulation efficiency, we measured X-ray magnetic circular dichroism (XMCD) using soft and hard X-rays at SPring-8 **BL25SU** and **BL39XU**, respectively. The film used for these measurements was a Pt/$Cr_2O_3$ bilayer because the thick bottom Pt layer masked the tiny signal from the top Pt. Figure 2 shows the X-ray absorption spectrum (XAS) and XMCD spectrum at the Cr $L_{2,3}$ edges and Pt $L_3$ edge. A magnetic field was applied perpendicular to the film plane to define the AFM spin orientation. XAS at the Cr $L_{2,3}$ edges indicates that the valence state of Cr was trivalent, $Cr^{3+}$. The clear XMCD signal indicates the presence of spin-polarized $Cr^{3+}$ which agrees with the BM prediction. Sum-rule analysis with the spin-correction factor gives the effective spin magnetic moment and orbital magnetic moment per $Cr^{3+}$ as $m_{s\_eff}$ = 0.016 ± 0.007 $\mu_B$ and $m_{orb}$ = 0.006 ± 0.004 $\mu_B$, respectively. The $m_{orb}/m_{s\_eff}$ value was 0.3 ± 0.3, which is comparable to that of an FM-based system with a low $\Delta\mu_0 H_{SW}/\Delta V_G$. No appreciable XMCD signal was observed at the Pt $L_3$ edge, suggesting that the alternative mechanism of the VCMA effect was inappropriate for the observed giant modulation efficiency. First-principles calculations revealed that the VCMA effect at the Pt/$Cr_2O_3$ interface was comparable to that in the FM cases, which supports the idea that the ME effect is the main mechanism of the giant modulation of the switching field.

Finally, we demonstrate a novel functionality based on the ME effect. According to the ME effect, the Zeeman energy gain of *E*-induced *M* is expressed as $\alpha EH$. Because of the sign $\alpha$ coupled with the AFM order parameter, the stable AFM spin state is determined by the sign of the *EH* product. Figure 3 plots $\mu_0 H_{SW}$ as a function of *E*. In the figure, the stable spin states are denoted by painted areas. Two hyperbolas corresponding to $\alpha EH$ = constant with positive and negative $\alpha$ values were observed. The four painted areas outside the hyperbola show monostable regions. The presence of these areas indicates that deterministic access to any of the four quadrants is possible, which is the principle of the logic-operation. The yellow area indicates a bistable region inside the hysteresis shown in Fig. 1(b), which works as the memory function of the device. These functionalities shed light on the ME-AFM materials, and our demonstration will advance the field of voltage-based AFM spintronics.

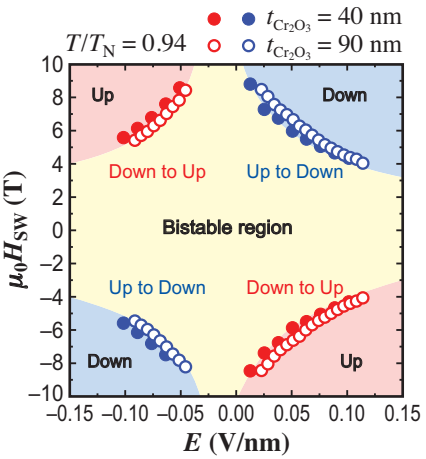


Fig. 3. *E*-dependence of switching field exhibiting the four quadrants access of the AFM spin state. Up and down shown in the red and blue painted areas are denoted by the sign of $R_{xy}$ shown in Fig. 1(b).

Yu Shiratsuchi

Graduate School of Engineering, Osaka University

Email: shiratsuchi@mat.eng.osaka-u.ac.jp

**References**

[1] K. D. Belashchenko: Phys. Rev. Lett. **105** (2010) 147204.
[2] T. Moriyama *et al.*: Phys. Rev. Appl. **13** (2020) 034052.
[3] *K. Ujimoto, H. Sameshima, K. Toyoki, T. Moriyama, K. Nakamura, Y. Kotani, M. Suzuki, I. Iino, N. Kawamura, R. Nakatani and Y. Shiratsuchi: NPG Asia Mater. **16** (2024) 20.*